Supplementary Information

Low-Cost Optodiagnostic for Minute-Timescale Detection of SARS-CoV-2

André Lopes Ferreira[1-4], Lucas Felipe de Lima[1-4], Marcelo Der Torossian Torres[1-3], William Reis de Araujo[4,], and Cesar de la Fuente-Nunez[1-3,*]*

[1]Machine Biology Group, Departments of Psychiatry and Microbiology, Institute for Biomedical Informatics, Institute for Translational Medicine and Therapeutics, Perelman School of Medicine, University of Pennsylvania, Philadelphia, Pennsylvania 19104, United States of America.

[2]Departments of Bioengineering and Chemical and Biomolecular Engineering, School of Engineering and Applied Science, University of Pennsylvania, Philadelphia, Pennsylvania 19104, United States of America.

[3]Penn Institute for Computational Science, University of Pennsylvania, Philadelphia, Pennsylvania 19104, United States of America.

[4]Portable Chemical Sensors Lab, Department of Analytical Chemistry, Institute of Chemistry, State University of Campinas - UNICAMP, Campinas, SP 13083-970, Brazil.

CONTENTS:

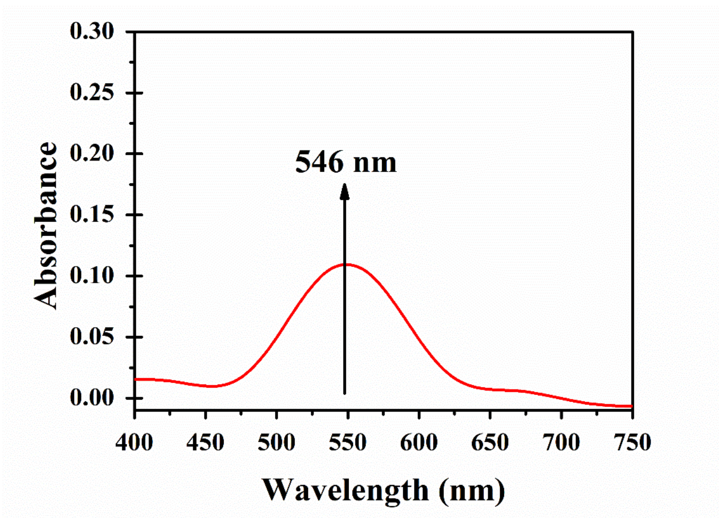

Figure S1. UV-Vis spectrum of the synthesized AuNano-cys. The AuNano-cys suspension presented a maximum absorbance at 546 nm, which is characteristic of the plasmonic effect of gold nanoparticles. Therefore, this wavelength was used to study the long-term stability of AuNano-cys (Figure S2).

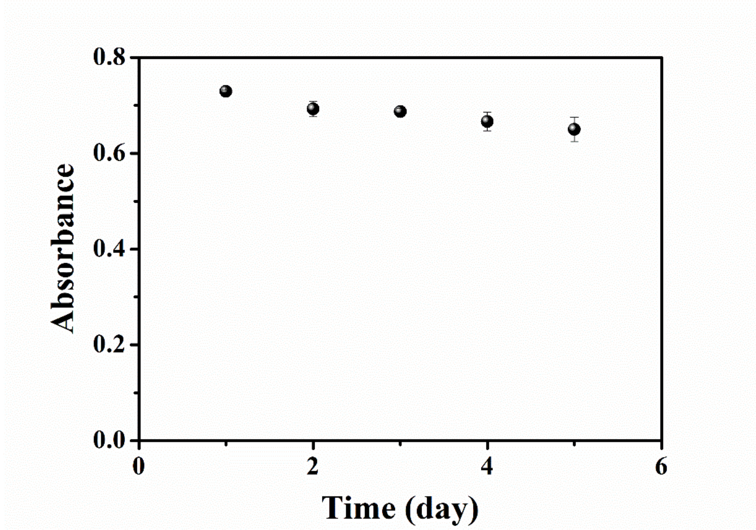

Figure S2. Stability study of the AuNano-cys solution. The stability study was evaluated by considering the mean values of the absorbance band at 546 nm extracted from UV-Vis spectra recorded over 5 days. The solution was stored at 4 ºC in a light-protected environment. Note that the AuNano-cys presented adequate stability along the period evaluated.

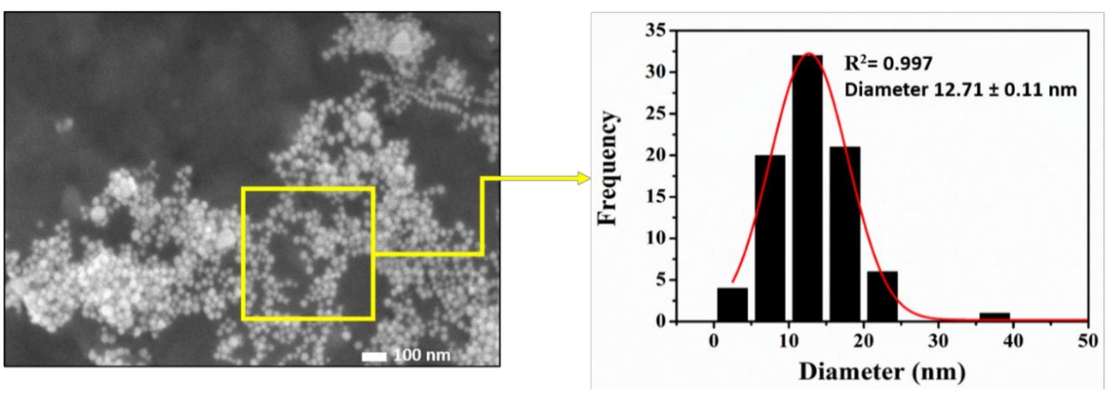

Figure S3: SEM image characterization of the AuNano-cys-ACE2 in the absence of SARS-CoV-2 SP. The functionalized nanoparticles presented a spherical shape with a mean diameter size of 12.71 ± 0.11 nm with a determination coefficient (R^2) of 0.997.

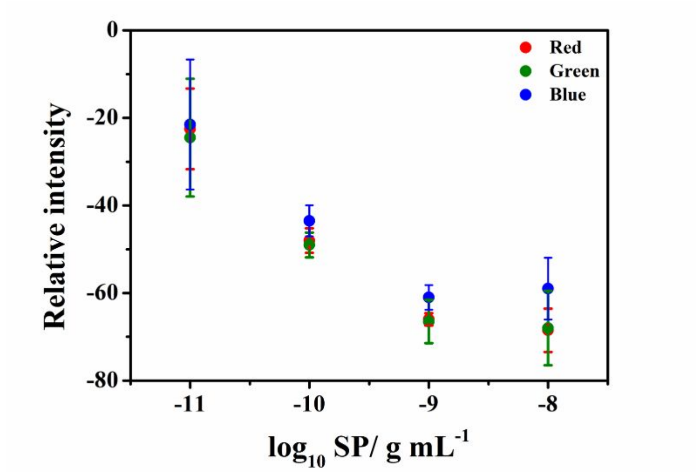

Figure S4: Analytical curve comparison using Red (R), Green (G), and Blue (B) color patterns. The analytical curves were built in triplicate (n=3) using SP at concentrations ranging from $1x10^{-11}$ g mL^{-1} to $1x10^{-8}$ g mL^{-1}. A linear behavior was observed at concentrations ranging from $1x10^{-11}$ g mL^{-1} to $1x10^{-9}$ g mL^{-1} of SP for relative intensity of red, green, and blue colors.

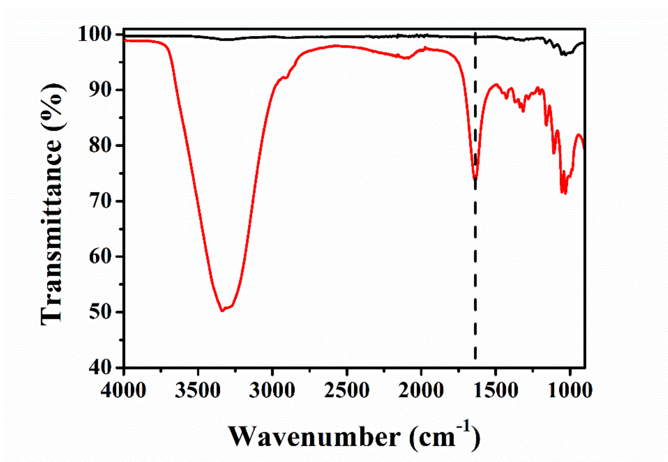

Figure S5. FTIR characterization of the cotton swab activation process. FTIR was used to evaluate the effectiveness of the cotton surface activation protocol. The cotton swab was immersed in a 2.0 mmol L^{-1} potassium periodate (KIO_4) solution containing 1.0 mL sulfuric acid overnight at room temperature to generate aldehyde functional groups to enable the subsequent covalent immobilization of ACE2 to the cotton swab surface through the formation of an amide bond between the activated cotton and the enzyme using EDAC:NHS. Note that the FTIR spectrum of the cotton swab after the activation process with potassium periodate (red line) shows a clear enhanced signal of the band at 1654 cm^{-1}, characteristic of the carbonyl group, compared to the spectrum obtained for the non-activated cotton swab (black line), confirming the successful generation of aldehyde functional groups [1].

Table S1. Diagnosis of 100 NP/OP samples from inpatients at the Hospital of the University of Pennsylvania (HUP) with COVID-19 symptoms using COLOR (COVID-19 Low-cost Optodiagnostic for Rapid testing). All samples were determined as COVID-19 positive or negative by RT-PCR.

Viral Load	NP/OP Sample ID	COVID-19 Status	RT-PCR	COLOR	Ct	$R\text{-}R_0$
High	**7**	positive	+	+	19.2	-71
	60	positive	+	+	20	-62
	63	positive	+	+	20	-60
	24	positive	+	+	20.6	-56
	28	positive	+	+	20.7	-55
	74	positive	+	+	21.1	-55
	40	positive	+	+	21.5	-52
	38	positive	+	+	21.8	-50
	16	positive	+	+	22.2	-48
	51	positive	+	+	22.3	-47
	8	positive	+	+	22.8	-45
	54	positive	+	+	22.9	-44
	39	positive	+	+	23	-44
	3	positive	+	+	23.3	-44
	50	positive	+	+	23.4	-44
	27	positive	+	+	24.2	-44
	29	positive	+	+	24.2	-41
	44	positive	+	+	24.2	-39
	59	positive	+	+	24.8	-36
Intermed iate	**20**	positive	+	+	25.3	-36
	2	positive	+	+	26.1	-36
	30	positive	+	+	26.1	-35
	11	positive	+	+	26.5	-35
	43	positive	+	+	26.5	-32
	34	positive	+	+	26.8	-32

	VTMSET-53	positive	+	+	27.1	-31
	33	positive	+	+	27.4	-30
	31	positive	+	+	28.2	-30
	VTMSET-56	positive	+	+	28.7	-29
	VTMSET-60	positive	+	+	28.8	-29
	VTMSET-06	positive	+	+	29.2	-29
	VTMSET-04	positive	+	+	29.4	-27
	47	positive	+	+	30	-27
LOW	**26**	positive	+	+	30.1	-26
	4	positive	+	+	30.4	-26
	VTMSET-40	positive	+	+	30.5	-25
	VTMSET-33	positive	+	+	30.7	-25
	53	positive	+	+	31.2	-24
	32	positive	+	+	31.9	-22
	VTMSET-59	positive	+	+	31.9	-21
	1	positive	+	+	32.1	-21
	52	positive	+	+	32.2	-20
	VTMSET-26	positive	+	+	32.3	-19
	25	positive	+	+	32.5	-15
	65	positive	+	+	32.5	-14
	18	positive	+	+	32.8	-14
	VTMSET-25	positive	+	+	33	-13
	46	positive	+	+	33.6	-10
	5	positive	+	-	34.3	-1
	15	positive	+	-	35.4	4
Negative Samples	**VTMSET-07**	negative	-	-	-	1
	VTMSET-21	negative	-	-	-	13
	VTMSET-35	negative	-	-	-	1
	VTMSET-46	negative	-	-	-	5
	VTMSET-55	negative	-	-	-	7
	VTMSET-57	negative	-	-	-	5

	VTMSET-58	negative	-	-	-	13
	VTMSET-61	negative	-	-	-	11
	VTMSET-69	negative	-	-	-	3
	VTMSET-70	negative	-	-	-	5
	VTMSET-265	negative	-	-	-	-6
	VTMSET-266	negative	-	-	-	-4
	VTMSET-267	negative	-	+	-	-12
	VTMSET-268	negative	-	-	-	-5
	VTMSET-269	negative	-	+	-	-11
	VTMSET-270	negative	-	-	-	-2
	VTMSET-271	negative	-	-	-	-8
	VTMSET-272	negative	-	-	-	-1
	VTMSET-273	negative	-	-	-	-2
	VTMSET-274	negative	-	-	-	-5
	VTMSET-275	negative	-	-	-	-7
	VTMSET-276	negative	-	-	-	-6
	VTMSET-277	negative	-	-	-	-8
	VTMSET-278	negative	-	-	-	-5
	VTMSET-279	negative	-	-	-	-5
	VTMSET-280	negative	-	-	-	-6
	VTMSET-281	negative	-	-	-	-4
	VTMSET-282	negative	-	+	-	-17
	VTMSET-283	negative	-	-	-	1
	VTMSET-284	negative	-	+	-	-11
	VTMSET-285	negative	-	+	-	-24
	VTMSET-286	negative	-	-	-	0
	VTMSET-287	negative	-	-	-	-7
	VTMSET-288	negative	-	-	-	-6
	VTMSET-289	negative	-	-	-	-9
	VTMSET-290	negative	-	-	-	-3
	VTMSET-291	negative	-	-	-	-8

	VTMSET-292	negative	-	+	-	-24
	VTMSET-293	negative	-	-	-	1
	VTMSET-294	negative	-	-	-	-9
	VTMSET-295	negative	-	-	-	-4
	VTMSET-296	negative	-	-	-	-5
	VTMSET-297	negative	-	+	-	-11
	VTMSET-298	negative	-	-	-	-4
	VTMSET-299	negative	-	-	-	-4
	VTMSET-300	negative	-	-	-	2
	VTMSET-301	negative	-	-	-	-4
	VTMSET-302	negative	-	-	-	-9
	VTMSET-303	negative	-	-	-	-7
	VTMSET-304	negative	-	+	-	-25

Please note that, among the 15 SARS-CoV-2 RT-PCR positive samples with Ct values ranging from 30.5 to 35.4 (low viral loads), the R-R_0 values obtained ranged from -25 to 4. COLOR misdiagnosed only 2 samples with Ct values higher than 33.6 (Table S1). Out of the 8 SARS-CoV-2 RT-PCR negative samples that COLOR misinterpreted as positive samples (*i.e.*, false positives), the R-R_0 values ranged from -25 to -11 (Table S1), highlighting the challenge represented by defining the appropriate cut-off value of a given diagnostic method. For example, if we define the cut-off value as R-$R_0 \leq -26$ (for SARS-CoV-2 positive results) COLOR would yield no false positive results; however, its sensitivity would decrease to 70% (35/50).

Supplementary reference

(1) Łojewska, J.; Miśkowiec, P.; Łojewski, T.; Proniewicz, L. M. Cellulose Oxidative and Hydrolytic Degradation: *In Situ* FTIR Approach. *Polym. Degrad. Stab.* **2005**, *88* (3), 512–520. https://doi.org/10.1016/j.polymdegradstab.2004.12.012.